

# Membership Privacy Evaluation in Deep Spiking Neural Networks

Jiaxin Li\*  
University of Padua  
Padova, Italy  
jiaxin.li@studenti.unipd.it

Gorka Abad  
Radboud University  
Nijmegen, Netherlands  
abad.gorka@ru.nl

Stjepan Picek  
Radboud University  
Nijmegen, Netherlands  
stjepan.picek@ru.nl

Mauro Conti  
University of Padua  
Padova, Italy  
conti@math.unipd.it

**Abstract**—Artificial Neural Networks (ANNs), commonly mimicking neurons with non-linear functions to output floating-point numbers, consistently receive the same signals of a data point during its forward time. Unlike ANNs, Spiking Neural Networks (SNNs) get various input signals in the forward time of a data point and simulate neurons in a biologically plausible way, i.e., producing a spike (a binary value) if the accumulated membrane potential of a neuron is larger than a threshold. Even though ANNs have achieved remarkable success in multiple tasks, e.g., face recognition and object detection, SNNs have recently obtained attention due to their low power consumption, fast inference, and event-driven properties. While privacy threats against ANNs are widely explored, much less work has been done on SNNs. For instance, it is well-known that ANNs are vulnerable to the Membership Inference Attack (MIA), but whether the same applies to SNNs is not explored.

In this paper, we evaluate the membership privacy of SNNs by considering eight MIAs, seven of which are inspired by MIAs against ANNs. Our evaluation results show that SNNs are more vulnerable (maximum 10% higher in terms of balanced attack accuracy) than ANNs when both are trained with neuromorphic datasets (with time dimension). On the other hand, when training ANNs or SNNs with static datasets (without time dimension), the vulnerability depends on the dataset used. If we convert ANNs trained with static datasets to SNNs, the accuracy of MIAs drops (maximum 11.5% with a reduction of 7.6% on the test accuracy of the target model). Next, we explore the impact factors of MIAs on SNNs by conducting a hyperparameter study. Finally, we show that the basic data augmentation method for static data and two recent data augmentation methods for neuromorphic data can considerably (maximum reduction of 25.7%) decrease MIAs' performance on SNNs. Regardless, the accuracy of MIAs could still be between 51.7% and 66.4% with data augmentation, indicating data augmentation cannot fully prevent MIAs on SNNs.

**Index Terms**—Membership Inference Attack, Spiking Neural Network, Artificial Neural Network, Data Augmentation.

## I. INTRODUCTION

Artificial Neural Networks model the behavior of a neuron with non-linear functions. As large amounts of data are collected and computing capabilities are enhanced, ANNs, especially deep neural networks [1], demonstrate an amazing ability to solve real-world tasks like face recognition [2] and object detection [3]. The third generation of neural network models, Spiking Neural Networks [4], mimic the dynamics of a neuron in a way closer to the actual neurons in the

brain. Figure 1 shows the basic neuron models for ANNs and SNNs. For ANNs, the neuron collects weighted inputs from previous neurons, applies a non-linear function  $\sigma$  to the summed input, and continuously outputs an identical activation value if the input is the same over time. For SNNs, the neuron modifies its membrane potential  $V$  (and the rate of change) according to binary spikes from previous neurons in the current time step. It outputs a spike when the membrane potential exceeds a threshold  $V_{th}$ . If there are no spikes from previous neurons, the membrane potential will gradually reset to a low value to save energy. The neuron remains inactive until a new spike is received, which improves power consumption. Due to those properties and the development of neuromorphic devices (e.g., TrueNorth from IBM [5] and Loihi from Intel [6]), SNNs gained much attention in scenarios like the autonomous operation of the vehicle [7], industrial fault diagnosis [8], and healthcare diagnosis with biomedical signals [9], [10].

Since the initially proposed SNNs could be hard to train and usually perform worse than ANNs [4], [11], [12], many works follow lessons from ANNs to improve the performance of SNNs. Specifically, directly converting trained ANNs to SNNs [13], [14], [15], increasing the depth of the model [16], [17], replacing the non-differential threshold function with the differential surrogate function [18], and training SNNs with backpropagation [19]. Moreover, we can distinguish shallow and deep SNNs according to the number of layers within the structure of SNNs following the previous work [16], [17]. As deep SNNs could perform better than shallow SNNs [16], [17] and since they are used in real-world tasks [7], [20], our work focuses on deep SNNs trained with backpropagation or converted from ANNs.

Membership Inference Attacks, inferring whether a data point is in the training data of the target model, attract much attention in ANN research and practice, as indicated by recent laws like GDPR [21] and CCPA [22]. Applying SNNs in real-world tasks raises similar membership privacy concerns as in the case of ANNs. More precisely, being in the training data of SNNs could disclose the private information of users. For example, if the user's data is in the training data of the deep SNN trained for classification of Alzheimer's disease [23], we could infer that this user suffered from this disease if we know the data of this user is in the training data via MIA. As far as we know, no studies have evaluated the membership privacy

\*Corresponding author.

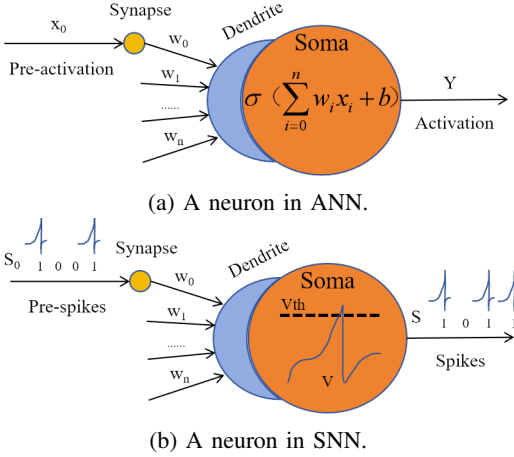


Fig. 1: Basic neuron model in ANNs and SNNs [12].

of deep SNNs. As such, we address this gap in our work.

Intuitively, MIAs on SNNs could be more challenging than MIAs on ANNs, considering a data point of the neuromorphic dataset consists of multiple frames, each of which is the accumulation of events that happen over a period. Let us consider the image classification task. A data point in the static dataset only contains one static image. A data point with multiple frames has more neighboring data points than the one with one static image. More neighboring data points make it harder to predict the existence of a specific data point, as the inclusion of neighboring data points could disturb the prediction of the MIA in this particular data point [24]. To solve this problem, we utilize spiking neurons' fire rate and membrane potential as signals of MIAs since they are cumulative results of multiple frames and could represent the prediction situation of multiple frames. In commonly used rate coding SNNs [25], the fire rate is a similar indicator to the confidence score to show the confidence of the prediction due to the alignment of Mean Squared Error (MSE) during training. Hence, we utilize previous strategies [26], [27], [28] in MIAs with confidence scores to MIAs with fire rates.

The membership evaluation results show that SNNs are more vulnerable than ANNs when training ANNs and SNNs with neuromorphic datasets. On the other hand, when working with static datasets, the vulnerability comparison between ANNs and SNNs depends on specific datasets. The conversion from ANNs to SNNs maximally reduces 11.5% on the performance of MIAs with a drop of 7.6% on the original classification task. In the hyperparameter study, we show that the ATan function and the Leaky Integrate and Fire (LIF) neuron bring a high classification accuracy with a large generalization gap, leading to MIAs' high attack accuracy. Next, the choices of Adam (with a learning rate of 0.001) and SGD (with a learning rate of 0.1) are suitable for training SNNs. Moreover, increasing the number of time steps will slightly increase the vulnerability under MIAs. Finally, the basic data augmentation method for static data and two recent data

augmentation methods for neuromorphic data could reduce MIAs' performance on SNNs by up to 25.7%. Unfortunately, the accuracy of MIAs could still be from 51.7% to 66.4% even when applied data augmentation.

Our main contributions are:

- 1) To the best of our knowledge, we are the first to evaluate the membership privacy of SNNs and compare their vulnerability to ANNs. We experiment with eight MIAs, six datasets, and three model structures, which lay the foundation for future work on the privacy of SNNs.
- 2) To understand MIAs on SNNs better, we investigate influential factors of MIAs during the training of SNNs in the hyperparameter study.
- 3) We apply data augmentation to defend against MIAs on SNNs. There, we show that the basic augmentation method for static datasets and two recent augmentation mechanisms for neuromorphic datasets can reduce but cannot completely prevent MIAs on SNNs.

Following the paper's acceptance, we will make our source code available to the community.

## II. BACKGROUND

In Section II-A, we introduce SNNs and three main methods to build SNNs. Next, we give a simple explanation of the pipeline of MIAs in Section II-B.

### A. Spiking Neural Network

An SNN is an application of the biological neuron into AI for efficient and low-cost computation. There are three main methods to train SNNs.

**(1) Spike-Timing Dependent Plasticity (STDP).** For a pair of presynaptic and postsynaptic neurons, the synaptic weight of the synapse between those two neurons alters according to the arrival time of spikes from the presynaptic neuron and the firing time of the postsynaptic neuron. As an example, we consider a neuron "A" and a neuron "B" to be connected. The faster "A" fires, the stronger the connection with "B", and vice versa; when "A" does not fire as much, the connection is weakened. The weight will increase if the presynaptic neuron fires early and the postsynaptic neuron fires later. The weight will decrease if the presynaptic neuron fires later while the postsynaptic neuron fires early.

However, we do not consider this strategy because STDP is suitable for shallow SNNs. For deep SNNs, finding suitable hyperparameters and training with STDP is difficult, as mentioned in the previous work [29]. Our focus is deep SNNs, and we obtain deep SNNs trained via backpropagation or converted from ANNs.

**(2) Conversion from ANN.** Under this strategy, a pre-trained ANN is converted to an SNN by replacing the ReLU activation layers (that are not used in SNNs) with spiking neurons and adding scaling operations like weight normalization and threshold balancing [13], [14], [18], [30], [15]. Cao et al. [13] proposed using the absolute values of negative activations, changing Tanh to ReLU, removing biases, and using spatial linear subsampling instead of max-pooling. Diehl

et al. [14] further analyzed performance loss and suggested weight normalization methods to address the over- and under-activation of spiking neurons. Instead of applying the ReLU activation function while training an ANN, Hunsberger et al. [18] used a modified non-linearity LIF neuron and injected noise during training, improving the robustness of the converted SNN's approximation errors. Rueckauer et al. [30], [15] addressed approximation errors between spiking neuron fire rates and ANN activations, which degrade the accuracy of deep models, by resetting potentials through subtraction and retaining biases as constant input currents scaled by maximum ReLU activation.

In our experiments to attack converted SNNs with MIAs, we follow previous works [30], [15]: i) reset the potential by subtraction (the membrane potential threshold  $V_{th} = 1.0$ ), ii) re-scale weights and biases with the robust normalization ( $p = 99.9\%$ ), iii) achieve batch normalization via scaling weights and biases, and iv) directly feed the input to the converted SNN, and pass the output through a softmax function. We do not consider max-pooling because it requires estimating presynaptic firing rates, which is computationally complex [30] and does not give much benefit. Hence, we follow the strategy of average pooling from the work of Dieh et al. [14].

**(3) Backpropagation-based supervised learning.** Under this strategy, we train SNNs via backpropagation, the same way as training ANNs. Among various neural models [31], [32], the Leaky Integrate and Fire (LIF) model can mimic the behavior of the biological neuron with a minimum number of circuit elements [33] and bring a lower complexity. As LIF is frequently used in previous works [34], [19], [35], we utilize the LIF model as well. The membrane potential of a spiking neuron  $i$  under the LIF model is formulated as given in Eqs. (1) and (2). In Eq. (1),  $V_{rest}$  is the membrane potential of a neuron without any input. We set  $V_{rest}$  as 0 following the related work [35].  $V(t)$  is the membrane potential of neuron  $i$  at time  $t$ .  $\tau$  is the membrane time constant. In Eq. (2), the neuron  $i$  has  $n_i$  presynaptic neurons. For a presynaptic neuron  $j$ , it has a list of spiking times  $t_j^{pre}$ ,  $w_{ij}$  is the synaptic weight between neuron  $i$  and a presynaptic neuron  $j$ , and  $\delta(t)$  is the Dirac delta function (if  $t \neq 0$ ,  $\delta(t) = 0$ .  $\int_{-\infty}^{\infty} \delta(t)dt = 1$ ).

$$\tau \frac{dV(t)}{dt} = -(V(t) - V_{rest}) + X(t). \quad (1)$$

$$X(t) = \sum_{j=1}^{n_i} \sum_{t_s^{pre} \in t_j^{pre}} w_{ij} \delta(t - t_s^{pre}). \quad (2)$$

To consider  $V(t)$  in discrete time, we obtain Eq. (3) after applying the Euler method to Eq. (1).

$$H(t) = V(t-1) + \frac{1}{\tau}(-(V(t-1) - V_{rest}) + X(t)). \quad (3)$$

Apart from the neuronal dynamics, the neuron will elicit a spike  $S(t)$  to the subsequent neurons if the membrane potential is larger than a threshold  $V_{th}$ , which is formulated in Eq. (4).

After eliciting a spike, the membrane potential  $V(t)$  will be reset as  $V_{reset}$  as explained in Eq. (5).

$$S(t) = \begin{cases} 1 & \text{if } H(t) \geq V_{th}, \\ 0 & \text{others.} \end{cases} \quad (4)$$

$$V(t) = H(t)(1 - S(t)) + V_{reset}S(t). \quad (5)$$

To apply backpropagation to the training of SNN, it is a common practice to keep  $S(t)$  for the forward pass and replace  $S(t)$  with a differentiable surrogate function to calculate the backward gradient of the backpropagation as  $S(t)$  is not differentiable [36]. Among potential surrogate functions, we set Atan as the default one as the performance of the original task is higher than applying other explored surrogate functions, as shown in the hyperparameter study in Section V-B. The Atan function is formulated as Eq. (6), where Eq. (7) is its gradient.  $\alpha$  is the pre-defined parameter with a default value of 2.0, following the implementation of SpikingJelly [37].

$$S(t) = \frac{1}{\pi} \arctan\left(\frac{\pi}{2} \alpha H(t)\right) + \frac{1}{2}. \quad (6)$$

$$\frac{\partial S(t)}{\partial H(t)} = \frac{\alpha}{2(1 + (\frac{\pi}{2} \alpha H(t))^2)}. \quad (7)$$

In the forward computation of each frame within the model, SNN aligns the spiking outputs to the one-hot encoding representation of the target category to make the spiking neuron belonging to the target category output a spike while other neurons do not. An MSE loss is calculated according to the matching degree of the spiking output and the one-hot encoding representation. The optimization guided by the MSE loss via Adam [38] or SGD [39], standard optimization algorithms in ANNs, implements the alignment by updating the weights.

### B. Membership Inference Attack

MIAs try to infer if a data point has been used during a target model's training by analyzing it or by observing its behavior to arbitrary inputs. Since the first works of MIA in machine learning [26], [27], many works have investigated MIAs with different adversary knowledge [40], [41], [42], [43], various model types [44], [45], [46], and distinct attack methods [47], [24], [28], [48], [49]. Formally, MIA is formulated as a function  $A : x, M, \Omega \rightarrow \{0, 1\}$  with a data point  $x$ , the target model  $M$ , and external knowledge  $\Omega$  of the adversary. The output 1 means that  $x$  is a member of  $M$ 's training data and 0 otherwise.

Currently, there are two main strategies for implementing MIAs: classifier-based and threshold-based methods. In classifier-based methods, the adversary trains the attack model, a classifier, to predict whether a data point is a member based on features (e.g., the confidence scores [26]) extracted from this data point from the target model. The adversary trains a shadow model to mimic the target model's behavior. The adversary does not have access to the original training data but to some data with a similar distribution to the original.

Then, the adversary constructs an attack model by using a dataset extracted from the features obtained by querying the shadow model.

For the threshold-based methods, the adversary directly compares a data point's metric (e.g., loss [47]) with a threshold to predict its membership. Usually, this threshold is determined according to the average value of the metric in the training data or is selected as the one that obtains high performance on the metric values of the shadow model.

### III. MEMBERSHIP PRIVACY EVALUATION

In this part, we define a data point in the neuromorphic dataset and the input and output of the SNN in Section III-A. In Section III-B, we provide the threat model. Section III-C explains the methods with detailed metrics to evaluate the membership privacy of SNNs.

#### A. Definitions

A data point in the training data of SNNs differs from a data point in the training data of ANNs. Let us take the image classification task as an example. A data point used for training ANNs is a three-dimensional (RGB) array, each of which is a pixel value (after normalization) ranging from 0 to 1. In rate coding SNNs, a data point is a list of time-series events measuring the brightness change during the relative movement between the object (or its image) and the Dynamic Vision Sensor (DVS) camera. The DVS camera will generate a positive polarity event with coordinate information if the brightness of a pixel increases over a threshold. If the brightness decreases below a threshold, the DVS camera will generate a negative polarity event with coordinate information. Hence, there are two types of events, categorized in two dimensions (positive and negative), in the list of events that belong to a data point. In neuromorphic datasets from SpikeJelly [37], a list of time-series events is accumulated into a fixed number (i.e., time steps) of frames for each data point. This indicates a data point of SNNs is a fixed number of frames.

Instead of inferring the membership of one static image in ANNs, MIAs on SNNs need to consider the membership of multiple static images (frames). A data point with multiple static images has more neighboring data points than one with one static image. More neighboring data points make it harder to predict the existence of a specific data point, as the inclusion of neighboring data points could disturb the prediction of MIA [24]. To solve this problem, we utilize the fire rate of spiking neurons and the membrane potential as the features. The reason for selecting the fire rate is that the fire rate contains the spiking outputs of multiple frames of a data point rather than the spiking output of one step. Hence, the fire rate is suitable for representing the prediction towards multiple frames. As for the membrane potential, the forward of one frame in the SNN will modify the membrane potential of neurons in the SNN, and the accumulation of membrane potential on multiple frames represents the prediction situation of multiple frames to a certain extent. Hence, we choose the fire rate and the membrane potential as the features.

For a data point  $x \in R^{T \times 2 \times H \times W}$  ( $T$ , 2,  $H$ , and  $W$  are the time steps, positive and negative channels, height, and width of the input), the target SNN  $M$  outputs the spiking times among  $T$  steps as  $M(x) \in R^{T \times n}$  ( $n$  is the number of classification categories), each of which represents whether a spiking neuron evokes a spike at current time spot. Therefore, the fire rates of  $M$  on  $x$  is  $Fr(x) = \frac{\sum_{t=1}^T M(x)_t}{T} \in R^n$  and  $M(x)_t \in R^n$  is spiking times at time spot  $t$ . For the last layer composed of spiking neurons (the number of neurons is  $m$ ), the membrane potential of spiking neurons for  $x$  is  $Mp(x) \in R^{T \times m}$ . Therefore, the average membrane potential among  $T$  time steps is  $AMp(x) = \frac{\sum_{t=1}^T Mp_t(x)}{T}$  and  $Mp_t(x) \in R^m$  is the membrane potential at time step  $t$ . We utilize fire rates and average membrane potential of the target SNN  $M$  on a data point as the signal to predict its membership.

#### B. Threat Model

Following the common practice of MIA [26], the adversary holds a shadow dataset from the same distribution as a target dataset used for training and testing the target SNN  $M$ . There are no overlapping data points between the shadow and target datasets. The adversary knows  $M$ 's hyperparameters and model structure to train a shadow SNN  $M_s$  for mimicking  $M$ , following previous works [26], [28]. Controlling the training and test data of  $M_s$ , the adversary can extract attack features from the training and test data of  $M_s$  by feeding data into  $M_s$  and label features as members (from training data) and non-members (from test data) separately. With the attack features and corresponding labels, the adversary trains a classifier or determines a threshold for distinguishing members and non-members. With the classifier (attack model) or threshold, the adversary evaluates the performance of MIA on the target SNN  $M$ . For attack features, we assume the adversary knows the fire rates  $Fr(x)$  and the average membrane potential  $AMp(x)$  of a data point  $x$  to evaluate the membership privacy of  $M$  under various MIAs. Finally, the adversary knows the loss, prediction label, and ground truth  $y$  of  $x$ , following the assumptions in previous MIAs on ANNs [26], [47].

#### C. Methodology

We follow strategies of previous MIAs (with confidence scores) on ANNs to leverage fire rates to implement MIAs on SNNs. The reason is that the fire rate is a similar indicator to the confidence score to show the confidence of the prediction. The training of backpropagation-based SNNs aligns the spiking neurons' output with the one-hot encoding representation of the target category with MSE. The alignment aims for SNN to only output a spike in the neuron belonging to the target category at each time step. Ideally, the fire rate of the neuron belonging to the target category is one, and other neurons have a fire rate close to zero. Hence, the fire rate reflects the SNN's confidence in the prediction of the data point. In the previous work [26], the ANN's prediction confidence gap on the training and test data makes MIAs feasible. Therefore, we follow previous strategies when handling confidence scores to use fire rates. We select five

representative methods in the field of MIA, including the first MIA on machine learning [26], two methods relaxing assumptions of MIA [27], the performance improvement with modified entropy (Mentr) [50], and performance improvement with logit-scaled confidence [28].

Apart from the five mentioned methods, we also choose two methods from the work of Yeom et al. [47]. One is the MIA based on loss, and the other is based on the prediction correctness. The reason for selection is that the loss of the training data tends to be lower than the loss of the test data after training, and the MIA based on prediction correctness provides a baseline method to directly infer the data points correctly predicted by the target model as the training data. To compare the vulnerability of MIAs on ANNs and SNNs, we apply those seven methods. For the average membrane potential, we take it as the feature of the attack model to directly infer the membership following the basic strategy in [26]. For MIAs on ANNs, we also evaluate hinge loss based on logits (the output before the softmax layer in the ANN) due to its more straightforward computation than the logit-scaled confidence and competitive performance [28].

In summary, we evaluate MIAs on SNNs with eight methods based on fire rates and membrane potential. For comparison, we implement eight MIAs on ANNs based on (1) confidence scores [26], (2) loss [47], (3) prediction correctness [47], (4) top-3 confidence scores [27], (5) maximum confidence score [27], (6) logit-scaled confidence [28], (7) hinge loss [28], and (8) Mentr with confidence scores [50]. For MIAs against SNNs, we discuss the details of each method as follows.

**(1) fire rates.** We take the fire rates  $Fr(x)$  of each data point as the feature of the attack classifier to predict the membership of each data point. **(2) loss.** We compare the single loss related to each data point with a threshold to determine its membership. The adversary evaluates MIAs on the shadow model and its training and test data to select the threshold that better distinguishes losses of training and test data of the shadow model.

**(3) prediction correctness.** If the target SNN  $M$  correctly predicts the classification label of  $x$ , we predict  $x$  is a member and non-member otherwise.

**(4) top-3 fire rates.** Instead of using all the fire rates, we select top-3 fire rates as the feature of the attack classifier, following the strategy in the previous work [27].

**(5) maximum fire rate.** We use the maximum fire rate to compare with a threshold. If the maximum fire rate exceeds the threshold, we predict  $x$  as member and non-member otherwise.

**(6) logit-scaled fire rate.** We compute the logit-scaled fire rate as Eq. (8), where  $Fr(x)_y$  is the fire rate of the spiking neuron of the ground truth. We replace the confidence score of logit-scaled confidence [28] with the fire rate to obtain this metric. Similarly, we compare the logit-scaled fire rate with a threshold for the membership prediction.

$$\log(Fr(x)_y) - \log \sum_{y' \neq y} Fr(x)_{y'}. \quad (8)$$

**(7) Mentr with fire rates.** Following the Mentr with confidence scores in the previous work [50], we calculate the Mentr with fire rates as Eq. (9). We compare this metric with a threshold while deciding on a membership of  $x$ .

$$-(1 - Fr(x)_y) \log(Fr(x)_y) - \sum_{y' \neq y} Fr(x)_{y'} \log(1 - Fr(x)_{y'}). \quad (9)$$

**(8) average membrane potential.** Apart from fire rates, we utilize the average membrane potential as the feature of the attack classifier to predict membership. Similarly, we train the attack classifier with features extracted from the shadow model on its data.

#### IV. EXPERIMENTAL SETTINGS

We discuss the datasets used in our experiments in Section IV-A. Then, we discuss the ANN and SNN models in Section IV-B. In Section IV-C, we detail the settings of training models, including target, shadow, and attack models. Besides, we clarify the evaluation metric.

##### A. Datasets

We select three neuromorphic datasets, N-MNIST [51], CIFAR10-DVS [52], and N-Caltech101 [51], to explore MIAs against SNNs. For comparison, we choose corresponding static versions (i.e., MNIST, CIFAR10, and Caltech101) of those three datasets to train ANNs. Table I shows the shape of a batch of data points and the number of data points in each dataset. Among the numbers representing the shape, the  $T$ ,  $B$ , and the last two numbers separately indicate the time steps, batch size, and height and width of data points.

TABLE I: Statistical information of each dataset.

Dataset	Shape of a batch of data points	Number of data points
N-MNIST	$T \times B \times 2 \times 34 \times 34$	70,000
CIFAR10-DVS	$T \times B \times 2 \times 128 \times 128$	10,000
N-Caltech101	$T \times B \times 2 \times 180 \times 240$	9,146
MNIST	$B \times 3 \times 28 \times 28$	70,000
CIFAR-10	$B \times 3 \times 32 \times 32$	60,000
Caltech101	$B \times 3 \times 180 \times 240$ (resize)	9,146

We load neuromorphic datasets from SpikingJelly [37] and static datasets from Pytorch. For dividing the whole dataset into two sub-datasets for shadow and target models, we select 50% data points as the target model's sub-dataset (training and test) and the remaining 50% as the shadow model's sub-dataset (training and test). For N-Caltech101 and Caltech101, the platform does not already divide the training and test data. Thus, we sample 90% data points of each sub-dataset as the training data and the left 10% as the test data to ensure the training data of models. For the four remaining datasets, we will follow the data division of the platform to sample training and test data. Besides, we keep the same number of member and non-member data for training the attack model and evaluating the performance of MIAs on the target model.

Apart from training SNNs with neuromorphic datasets and ANNs with static datasets, we train ANNs with neuromorphic

datasets and SNNs with static datasets. In the work of Deng et al. [12], the authors trained ANNs with neuromorphic datasets and SNNs with static datasets to empirically compare their performance on the visual recognition task. Inspired by their work, we investigate the membership privacy of ANNs with neuromorphic datasets and SNNs with static datasets, considering the feasibility of training. For a batch of data points ( $R^{T \times B \times 2 \times H \times W}$ ) in the neuromorphic dataset, we follow the previous work [12] to normalize the accumulated spike times to the image pixel range (0 to 1 after normalization) by dividing by the maximum spiking time of each location in this batch of data points and labeling each frame of the data point as the same label. This means that we keep positive and negative channels in the neuromorphic dataset rather than inserting a full-zero channel to construct an RGB format image like the “play\_frame” function of SpikingJelly. This is done to reduce the memory consumption of training and keep the attack performance comparison of the SNN and ANN both trained with the neuromorphic dataset fair. For a data point from the static dataset, we repeat the image for time-step times and utilize the first few layers of the SNN to transfer the static image into spike events [35] rather than transferring with a Poisson encoder, which might incur variability in the firing of the network and impair its performance [15].

## B. Models

We select three model structures to train SNNs, including the model defined in the work of Fang et al. [35] (we denote it CNN for convenience), VGG11 [53], and ResNet18 [54]. The number of convolutional, downsampling, and fully connected layers (i.e.,  $N_{conv}$ ,  $N_{down}$ , and  $N_{fc}$ ) in CNN from the work of Fang et al. [35] is given in Table II. Each downsampling layer comprises  $N_{conv}$  convolutional layers and a max-pooling layer.  $N_{down}$  downsampling layers and  $N_{fc}$  fully connected layers make the final model. For N-Caltech101, we modified the model structure for DVS128 Gesture from [35] to fit the input size of N-Caltech101. For ANNs with structures of VGG11 and ResNet18, we replace the neuron formulated as a ReLU activation function with spiking neurons to construct the corresponding SNNs with structures of VGG11 and ResNet18. We keep the weights and connections between neurons. Considering that there are two input channels for the neuromorphic data and that the original input of VGG11 and ResNet18 is expected to have three channels, we add a convolutional layer to increase the number of channels (upsampling).

TABLE II: Number of different layers in a CNN.

Dataset	$N_{conv}$	$N_{down}$	$N_{fc}$
N-MNIST	1	2	2
CIFAR10-DVS	1	4	2
N-Caltech101	1	5	2

For the CNN originally defined for neuromorphic datasets in the work of Fang et al. [35], we modify the spiking neurons to artificial neurons with a ReLU activation function and change the input channel of the first convolutional layer to three

as the number of channels in the static data is three. It is the opposite process compared to modifying the ANN to the SNN. Note that instead of directly utilizing the previous CNN (like AlexNet [55]) to train on static datasets, we modify the CNN originally defined for neuromorphic datasets (SNN) to the CNN used for static datasets. This modification allows a fair comparison between SNNs trained with neuromorphic datasets and ANNs trained with static datasets. For conversion from ANNs to SNNs, we discussed the conversion operation in Section II-A.

For the classifier-based MIA, the attack model is a multi-layer perceptron (MLP) with 2 hidden layers, each with 64 neurons, following the previous work [43]. The single-value output of the MLP represents the probability of being predicted as a member.

## C. Settings and Evaluation Metric

For ANNs and SNNs trained with neuromorphic and static datasets, per default, we utilize the identical learning rate of 0.001, Adam optimizer, and batch size range from 2 to 16 due to the input size. For ANNs, the loss function is cross-entropy loss, while the loss function is Mean Squared Error (MSE) for SNNs. The number of epochs is 30, 50, and 60 for MNIST (N-MNIST), CIFAR-10 (CIFAR10-DVS), and Caltech101 (N-Caltech101), respectively. The default number of time steps for ANNs is 16. For the attack model, the optimization algorithm is Adam, with a learning rate of 0.001. The number of training epochs is 300, and the batch size is 32. We use the Binary Cross Entropy (BCE) to guide the training of the attack model. In the hyperparameter study in Section V-B, we explore the impact of the optimizer, learning rate, and time steps on the performance of target models and MIAs, as they are vital settings for training SNNs.

For the evaluation metric of MIAs, we follow the previous works [26], [28] and use the balanced accuracy as the comparison metric of MIAs.

## V. RESULTS AND DISCUSSIONS

We compare the performance of MIAs on ANNs and SNNs in Section V-A. Next, we provide a hyperparameter study in Section V-B. Finally, we evaluate the basic augmentation method for static datasets and two augmentation mechanisms for neuromorphic datasets as the defenses against MIAs in SNNs in Section V-C.

### A. MIAs on SNNs and ANNs

We first compare the vulnerability of SNNs and ANNs under MIAs. To make the comparison fair, we make the structures of SNNs and ANNs similar except for the neurons. The hyperparameters (time steps, learning rate, batch size, and dataset split) are identical when utilizing the same dataset. We do not leverage data augmentation or other techniques to improve the generalization of models here, as those techniques usually differ between ANNs and SNNs [56]. However, we explore how to defend against MIAs with data augmentation



mechanisms by improving the generalization of models in Section V-C.

Figures 2 and 3 show the highest accuracy of eight MIAs and the performance of the original classification task under target models for three static and three neuromorphic datasets. In the left subfigure, the x-axis represents the highest balanced accuracy among eight MIAs, and the y-axis indicates the model type, among which conversion means the ANN is converted to SNN. In the right subfigure, the x-axis represents the accuracy of the original classification task, and the y-axis represents the model type. We show the accuracy of the original task via the target test accuracy and target generalization gap, which is target training accuracy minus target test accuracy. From previous works [47], [26], a higher generalization gap usually leads to a larger privacy leakage, i.e., a higher attack performance.

**Comparing the highest attack accuracy of MIAs among ANNs and SNNs under the same static dataset, we find vulnerability is related to the type of static dataset.** As the training data of the target model only occupy half of the original training data, the original classification accuracy of the target model is relatively lower than the accuracy reported in the previous work [35]. For MNIST, the highest attack accuracy of ANNs is similar to that of SNNs (around 50%) as the training and test accuracy of the target model is all above 99%, indicating almost no generalization gap. For CIFAR-10, the highest attack accuracy of ANNs is larger than that of SNNs, even though SNNs have a larger generalization gap than ANNs. For example, the SNN with a structure of ResNet18 has a generalization gap of 26.6% (larger than 18% with the ANN) and the highest attack accuracy of 69.4% (smaller than 72.9% with the ANN). We also observe this trend with CNN and VGG11 trained with CIFAR-10. Besides, the larger generalization gap does not always represent a higher attack performance under MIAs. The ANN with a lower generalization gap could have a higher attack accuracy than not only the SNN with a higher generalization gap but also the ANN with a higher generalization gap. This is an extension of previous findings [26], [28], [57] since they observed that ANN with a high generalization gap could have a low attack performance under MIAs. The ANN with a lower generalization gap could have a higher attack accuracy than not only the SNN with a higher generalization gap but also the ANN with a higher generalization gap. This is an extension of previous findings [26], [28], [57] since they observed that ANN with a high generalization gap could have a low attack performance under MIAs.

For Caltech101, MIAs obtain a higher attack accuracy on SNNs than ANNs. For example, the SNN with a structure of CNN has the highest attack accuracy of 74.1%, higher than 69.7% of the ANN. Similarly, MIAs have higher attack performance on SNN than ANN when the structure is ResNet18. While training different models with the same static dataset, the vulnerability comparison of SNNs and ANNs is consistent, which means the model type is not the factor that leads to the difference. Therefore, the dataset itself is the reason, corresponding with the previous work [57] that finds the dataset impacts the performance of MIAs. We notice the SNN with a structure of VGG11 has a low original classification accuracy (around 48%) and a negative generalization gap, which leads to the low performance of MIAs (52.3%). In summary, the vulnerability comparison between SNNs and

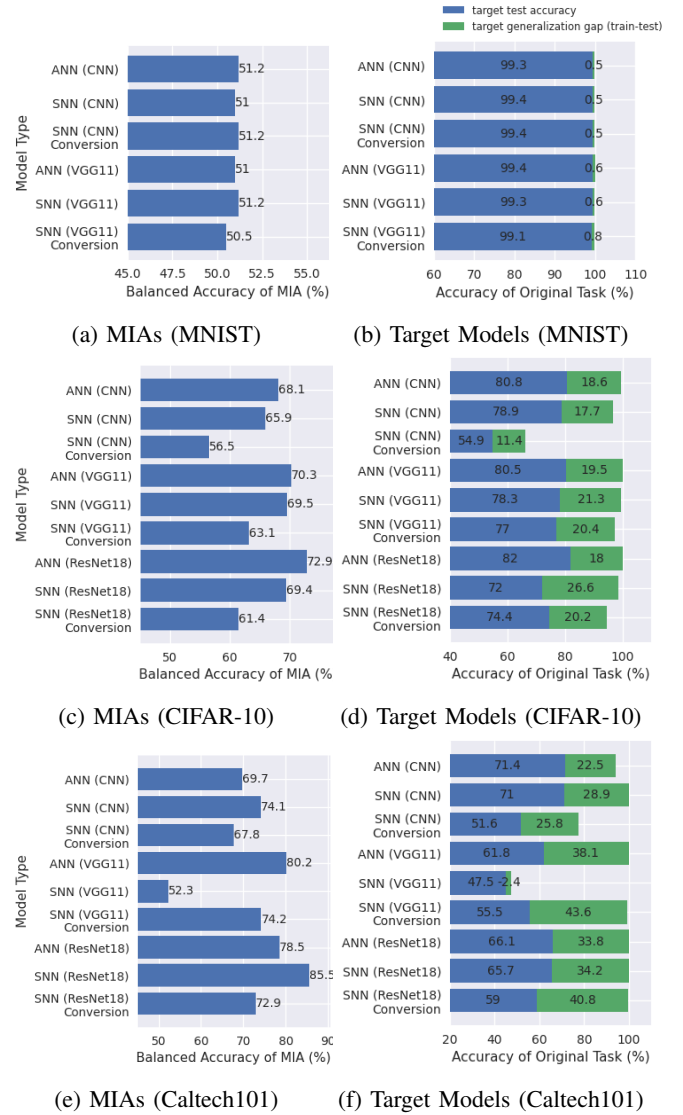


Fig. 2: The highest accuracy of eight MIAs, target test accuracy, and target generalization gap of three static datasets with various model types.

ANNs depends on the static datasets used for training ANNs and SNNs.

**Conversion from ANNs to SNNs reduces the performance of MIAs against converted SNNs with the accuracy drop on the original classification task.** For ANNs with a structure of CNN, the conversion to SNNs has a reduction of about 20% on the original classification accuracy on CIFAR-10 and Caltech101. The highest accuracy of MIAs drops from 68.1% to 56.5% (11.6%) for CIFAR-10 and from 69.7% to 67.8% (1.9%) for Caltech101. For VGG11 and ResNet18, converting from ANNs to SNNs brings an original classification accuracy drop within 8% (CIFAR-10 and Caltech101). However, the reduction of the highest attack accuracy could be larger than 10%. For example, the conversion from the ANN (ResNet18) with the highest attack accuracy of 72.9% to the

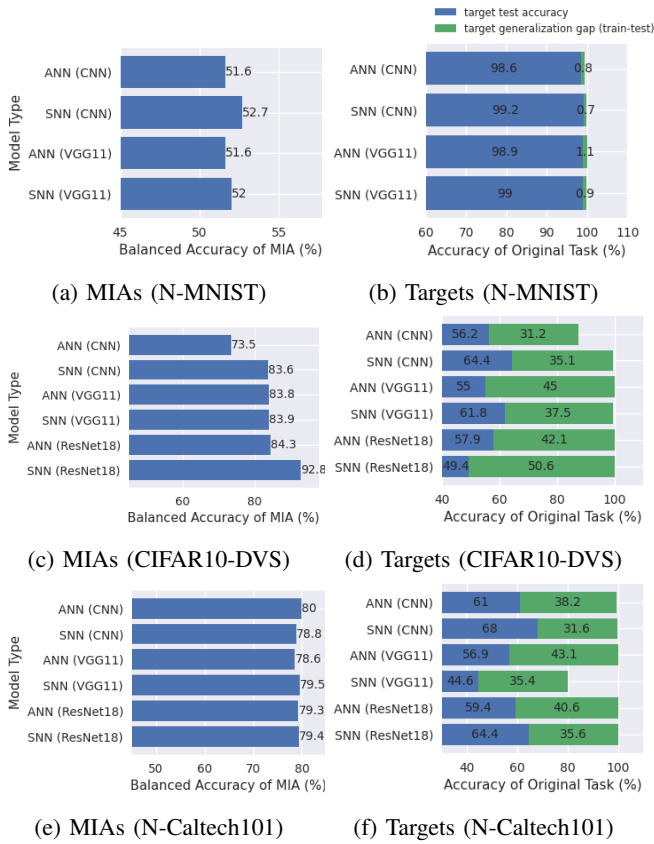


Fig. 3: The highest accuracy of eight MIAs, target test accuracy, and target generalization gap of three neuromorphic datasets with various model types.

SNN obtains a smaller highest attack accuracy of 61.4% (a reduction of 11.5%) with the original classification accuracy decreased from 82% to 74.4% (a reduction of 7.6%), even though the generalization gap increases from 18% to 20.2%. There are two reasons for the drop in MIAs' performance. The first reason is the decrease in performance of the original classification task and the generalization gap. The second is that converted SNN utilizes different neurons to connect weights and forward the input compared to the original ANN, which means a different way of weight utilization compared to the training of weights. As the weights are related to the training data and membership information, converted SNN loses part of the information due to the change of weight utilization, reducing the performance of MIAs and the original classification task. Since conversion from ANNs to SNNs could bring lower membership privacy leakage and a relatively low drop in the original task, we recommend the conversion to protect data points' privacy.

**When using neuromorphic datasets, SNNs are more vulnerable than ANNs due to the larger generalization gap.** For example, the SNN with a structure of ResNet18 trained with CIFAR10-DVS has a generalization gap of 50.6%, which is higher than 42.1% with the ANN. Under this condition, the highest accuracy of MIAs for the SNN is 92.8%, which is

higher than 84.3% with the ANN. With N-Caltech101, the highest accuracy of MIAs is similar for ANNs and SNNs. However, the generalization gaps of SNNs are smaller than those of ANNs. For example, the SNN with a structure of ResNet18 trained with N-Caltech101 has a generalization gap of 35.6%, which is smaller than 40.6% with the ANN. Nevertheless, the SNN and ANN have a similar highest attack accuracy of 79%. The SNN obtains a similar highest attack accuracy with a smaller generalization gap than the ANN, while the higher generalization gap usually leads to a higher attack accuracy. Hence, MIAs have a higher attack accuracy on SNNs than on ANNs due to a larger generalization gap or a similar attack accuracy on SNNs and ANNs if the generalization gap on SNNs is smaller than on ANNs. From the previous analysis, we conclude that the vulnerability of SNNs is higher than that of ANNs while being trained with neuromorphic datasets.

Figure 4 presents the relationship between the generalization gap and the highest accuracy among eight MIAs. As we can observe, the higher generalization gap usually leads to higher vulnerability under the MIAs, which corresponds to the conclusion from previous works [26], [47]. **This indicates the rule that a higher generalization gap of the target model usually leads to a higher vulnerability toward MIAs is still applicable for SNNs.**

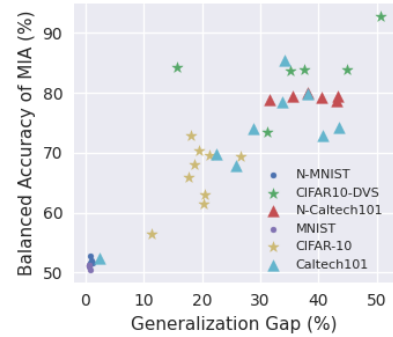


Fig. 4: The relationship between the generalization gap and the highest accuracy among eight MIAs.

We show the attack accuracy of eight MIAs in Appendices A and B. **From these two tables, we observe that loss, logit-scaled confidence (fire rate), and Mentr with confidence scores (fire rates) are the three metrics with higher accuracy among the metrics explored.** For example, both MIAs based on those three metrics obtain the highest accuracy of 78.6% against the ANN (VGG11) trained with N-Caltech101.

To investigate the modification of training loss and attack accuracy of MIAs along the training epochs, we apply MIAs against the trained model obtained after each epoch. Figure 5 in Appendix C shows how the loss, accuracy, and attack accuracy change during the training epochs of the target and shadow models. We consider the ANN and SNN based on CNN with CIFAR-10 and CIFAR10-DVS as examples. The



figure shows that the SNN has a stable test loss after reaching the minimum test loss. However, the test loss of the ANN will increase after arriving at the minimum test loss. The generalization gap increases during the training of ANNs and SNNs. Finally, the test accuracy becomes stable. As the optimization, the training accuracy still slowly increases with more epochs. **The accuracy of MIAs increases along the training epochs due to the increase of the generalization gap.**

### B. Hyperparameter Study

To explore the factors that impact the performance of MIAs on SNNs, we conduct a hyperparameter study to vary the spiking neuron type, surrogate function, optimizer, learning rate, and time steps during the training of SNNs.

#### 1) Varying Spiking Neuron Type and Surrogate Function:

For the backpropagation-based SNNs, we not only train the SNN with the LIF neuron type and the surrogate function of ATan to get the results in Table VIII but also explore other neuron types and surrogate functions. We select neuro-morphic datasets for training SNNs as examples to analyze the impact of spiking neuron type and surrogate function. We utilize three spiking neuron types (LIF, EIF [58], and Izhikevich [59]) and two surrogate functions (ATan and PiecewiseLeakyReLU [60]). The reason for selecting those three spiking neuron types and two surrogate functions is that they are common in the research of SNNs [58], [59], [60], [36], [11].

Table III provides the accuracy of the target model and the MIA with the highest accuracy under each setting. For N-MNIST, the SNN with PiecewiseLeakyReLU function and Izhikevich neuron is the most vulnerable one with the highest attack accuracy of 55.5%. For CIFAR10-DVS and N-Caltech101, SNNs with the ATan function and the LIF neuron have the highest attack accuracy (83.6% in CIFAR10-DVS and 77.6% in N-Caltech101) compared to other functions and neurons. This is mainly due to the larger generalization gap if the SNN is defined with the ATan function and the LIF neuron, even though the test accuracy is higher than that of other spiking neurons and surrogate functions.

2) *Varying Optimizer and Learning Rate:* As the selection of optimizer and learning rate impacts the generalization of the final trained model, we explore their influence on the final accuracy of SNNs and the performance of MIAs on SNNs. Table IV provides the accuracy of the target model and the MIA with the highest accuracy while training with different optimizers and learning rates. The table shows two settings unsuitable for training because their final classification accuracy is similar to random guessing, including Adam, with a learning rate of 0.1, and SGD, with a learning rate of 0.001. Indeed, the attack accuracy of MIAs is close to 50% under those two settings. For N-Caltech101, a higher generalization gap (35.4%) of the SNN trained with Adam and a learning rate of 0.001 leads to a higher attack accuracy of 79.5% compared to the SNN trained with SGD and a learning rate of 0.1. For CIFAR10-DVS, the SNN optimized with Adam and a

TABLE III: The attack accuracy under different spiking neuron types and surrogate functions while training SNNs (CNN).

Dataset	Surrogate Function	Spiking Neuron	Target Test Acc	Target Train Acc	MIA with Highest Acc	
					MIA	Acc
N-MNIST	ATan	LIF	99.2%	99.9%	fire rates	51.4%
	ATan	EIF	99.2%	99.7%	maximum fire rate	51.6%
	ATan	Izhikevich	98.8%	99.6%	loss	50.9%
	PiecewiseLeakyReLU	LIF	99.2%	99.9%	loss	51.7%
	PiecewiseLeakyReLU	EIF	99.1%	99.8%	loss	51.7%
	PiecewiseLeakyReLU	Izhikevich	98.8%	99.3%	Mentr with fire rates	55.5%
CIFAR10-DVS	ATan	LIF	66.4%	99.4%	loss	83.6%
	ATan	EIF	56.0%	82.0%	logit-scaled fire rate	69.2%
	ATan	Izhikevich	32.2%	30.8%	logit-scaled fire rate	53.3%
	PiecewiseLeakyReLU	LIF	62.6%	97.1%	loss	78.7%
	PiecewiseLeakyReLU	EIF	56.4%	68.5%	loss	61.3%
	PiecewiseLeakyReLU	Izhikevich	33.6%	29.6%	Mentr with fire rates	55.5%
N-Caltech101	ATan	LIF	69.9%	99.8%	loss	77.6%
	ATan	EIF	58.2%	86.5%	loss	69.0%
	ATan	Izhikevich	61.8%	81.8%	loss	64.3%
	PiecewiseLeakyReLU	LIF	41.6%	42.9%	loss	55.4%
	PiecewiseLeakyReLU	EIF	28.7%	27.7%	fire rates	53.0%
	PiecewiseLeakyReLU	Izhikevich	48.7%	48.8%	prediction correctness	58.3%

learning rate of 0.001 has a higher generalization gap (37.5%) than the SNN trained with the SGD and a learning rate of 0.1 (34.7%). However, MIAs have a smaller attack accuracy (83.9%) on the SNN trained with Adam and a learning rate of 0.001. This shows that a higher generalization does not always indicate a higher attack accuracy. From the training and test accuracy of SNNs with different optimizers and learning rates, we also observe that the training of SNNs is sensitive to those hyperparameters. A large (0.1) or a small learning rate (0.001) could both lead to the final trained SNN at the random guessing performance. The learning rate suitable for an optimizer might not be suitable for another optimizer, which indicates optimizers and learning rates should be considered together for training SNNs.

TABLE IV: The attack accuracy under different optimizers and learning rates while training SNNs (VGG11).

Dataset	Optimizer	LR	Target Test Acc	Target Train Acc	MIA with Highest Acc	
					MIA	Acc
CIFAR10-DVS	Adam	0.001	61.8%	99.3%	Mentr with fire rates	83.9%
	Adam	0.1	10.6%	9.8%	loss	50.0%
	SGD	0.001	10.0%	9.6%	loss	50.0%
	SGD	0.1	65.2%	99.9%	loss	88.8%
N-Caltech101	Adam	0.001	44.6%	80.0%	loss	79.5%
	Adam	0.1	9.2%	1.8%	loss	50.0%
	SGD	0.001	9.2%	4.2%	loss	50.0%
	SGD	0.1	63.4%	87.2%	loss	63.6%

3) *Varying the Number of Time Steps:* The number of time steps is an important factor for SNNs, as each data point

obtains the final prediction result based on the fire rate of the last spiking neurons during those steps. For each step, SNN takes one frame from a data point and updates the membrane potential of its spiking neurons to incur final spikes. We explore the impact of the number of time steps on the accuracy of target models and MIAs as shown in Table V. We observe that the gap between the highest attack accuracy obtained with time steps 8 and 16 is within 1%. For N-Caltech101, the attack accuracy under 4 time steps is higher due to a larger generalization gap. If we increase the number of time steps from 4 to 8, the highest attack accuracy will increase for N-MNIST and CIFAR10-DVS, even though the generalization gap slightly decreases with larger time steps. Hence, increasing the number of time steps would usually slightly increase the vulnerability towards MIAs to a certain stable level. We postulate the main reason for this phenomenon is that increasing the time steps means more frames of a data point will go through the model for updating its parameters, making the model have deeper memorization of the data point and, thus, MIA easier.

TABLE V: The attack accuracy with various time steps while training SNNs (CNN).

Dataset	The Number of Time Steps	Target Test Acc	Target Train Acc	MIA with Highest Acc	
				MIA	Acc
N-MNIST	4	98.7%	99.6%	loss	51.4%
	8	99.0%	99.9%	loss	52.3%
	16	99.2%	99.9%	loss	52.7%
CIFAR10-DVS	4	62.8%	98.1%	Mentr with fire rates	80.3%
	8	65.4%	99.3%	loss	83.7%
	16	64.4%	99.5%	loss	83.6%
N-Caltech101	4	61.4%	99.2%	loss	79.5%
	8	63.9%	99.6%	loss	78.0%
	16	68.0%	99.6%	logit-scaled fire rate	78.9%

### C. Defense Evaluation

Even though reducing the performance of MIA, Differential Privacy (DP) also causes a large utility loss, as demonstrated in the case of ANNs [26], [28]. Hence, we apply strategies for improving the generalization of SNNs to defend against MIAs. Indeed, the generalization gap is a commonly acceptable cause for MIAs [47], and the initial works [26], [27] also attempted to defend against MIAs with regularization and model ensemble. For neuromorphic datasets, we apply two strategies for data augmentation. The first strategy is EventDrop [61] to drop events in 1) a time interval, 2) an area of the coordinate, or 3) randomly. Following [61], we augment each data sample (a group of events) with the three mentioned dropping methods or do not augment them. The second strategy applies geometric augmentations (NDA [56]), including rolling, rotation, cutout [62], shear, flip, and CutMix [63]. Following the mechanism of “M1N2” in the original paper, we apply flip and CutMix and randomly select one of

the four left augmentation methods for each data sample. For static datasets, we apply basic strategies, including horizontal flip, random crop, and resize for data augmentation.

Tables VI and VII show the accuracy change of the target model and MIAs before and after applying data augmentation to static and neuromorphic datasets. From the two tables, we observe that data augmentation will reduce the target model’s generalization gap, leading to the performance drop of MIAs. For static datasets, SNNs trained with backpropagation reduce their generalization gap to a value close to 0 with data augmentation, leading to MIAs’ performance close to random guessing. Meantime, the test accuracy of the target model reduces 10% to 20%. The conversion of ANNs trained with data augmentation to SNNs decreases the accuracy of MIAs by about 10%, with the reduction of the test accuracy by more than 10%. Notably, the attack accuracy could also be as high as 66.4% while converting ANNs to SNNs. For ANNs trained with static datasets, the reduced accuracy of MIAs is still about 60%, which is 10% to 20% lower than the one without data augmentation, with about a 10% decrease in the generalization gap. The data augmentation for the static datasets prevents the SNNs trained with backpropagation from being attacked. For ANNs and SNNs converted from ANNs trained with static datasets, the data augmentation dramatically reduces the performance of MIAs.

Considering neuromorphic datasets and SNNs with a structure of VGG11, NDA [56] reduces the generalization gap to 6.9% for CIFAR10-DVS and 0.1% for N-Caltech101, which is smaller than the generalization gap with EventDrop [61] (29.5% for CIFAR10-DVS and 1.8% for N-Caltech101). Consequently, the performance of MIAs on SNNs trained with the NDA is lower than on SNNs trained with the EventDrop. For example, the attack accuracy of MIAs on the SNN (VGG11) drops from 83.9% to 58.3% while being trained with CIFAR10-DVS augmented with NDA. The attack accuracy is still 75.8% for the SNN (VGG11) with EventDrop. This indicates NDA is better than EventDrop in reducing the performance of MIAs. Besides, NDA maintains the test accuracy of SNN (VGG11) at 61.4%, which is slightly higher than the test accuracy of SNN (VGG11) with EventDrop (60.8%). For N-Caltech101, NDA reduces the performance of SNN (VGG11) to 53.8%, which is lower than 55.2% with EventDrop. The test accuracy of SNN (VGG11) is 35.2% and 32.0% with EventDrop and NDA. From the above analysis, we can observe that NDA is better than EventDrop in reducing the performance of MIAs. We believe that the geometric augmentations from NDA make the augmented data further from the original data, compared with the augmented data generated via randomly dropping events (EventDrop). Hence, NDA largely increases the generalization of the SNN and reduces the performance of MIAs.

For ANN (VGG11) trained with neuromorphic data, the performance of MIAs slightly increases even though the generation gap is smaller when the augmentation method is EventDrop. For example, the performance of MIA on ANN (VGG11) trained with CIFAR10-DVS increases from 83.8% to

86.5% after the application of EventDrop. While training the ANN on neuromorphic data, we accumulate events belonging to a data point into multiple frames and label each frame with the same class for training the ANN. Frames belonging to the same data point are similar as they describe the same object. The dropping of events reduces the dissimilarity between frames from the same data point, which leads to more similar frames. Those similar frames increase the memorization of the target model during training, causing the improvement of MIA. For the NDA augmentation method, the geometric augmentations make previous similar frames different and improve the target model’s generalization and test accuracy, reducing the performance of MIAs. For example, the accuracy of MIA drops from 83.8% to 71.8% with NDA, and the test accuracy increases from 55.0% to 63.7%. The above analysis further indicates that NDA is better at reducing the performance of MIA and even increasing the test accuracy of ANNs trained with neuromorphic data.

Basic augmentation on static data prevents SNNs trained with backpropagation from being attacked and reduces the performance of MIA on the SNNs converted from ANNs. Two augmentation methods on neuromorphic data decrease the performance of MIA on SNNs but cannot completely prevent them as the attack accuracy could also be 58.3% even for the effective augmentation mechanism, NDA. Moreover, the augmentation could lead to a drop in the test accuracy of the target model, reducing its utility. Therefore, the method to maintain the test accuracy and reduce the performance of MIAs could be an interesting future work.

## VI. RELATED WORKS

This part introduces previous works on MIA and attacks against SNNs.

### A. Membership Inference Attack

As people and governments pay more attention to personal data privacy, the development and research on MIA are flourishing, as discussed next. Since the successful membership inference attack in 2017 [26], the following works put much effort into ways to improve the performance of MIAs [27], [47], [28], [48], attacking strategies with less information [64], [42], [49], [43], MIAs on various datasets or models [46], [65], vulnerability of data points [66], [57], and defenses against MIAs [67], [68], [69].

Shokri et al. [26] proposed training multiple shadow models to mimic the behavior of the target model and extracting a dataset from the shadow model and its training and test data to train the attack model. Salem et al. [27] relaxed assumptions on the number of shadow models and the auxiliary data. Yeom et al. [47] proposed to utilize loss for MIA, and Ye et al. [48] enhanced MIAs based on loss with carefully designed thresholds.

Li et al. [64], and Choquette-choo et al. [42] leveraged the distance between the original data point and its black-box adversarial example as the signal of MIA. Hui et al. [49] eliminated shadow models by measuring the distance change

between the evaluation and non-member data to implement an MIA. Hayes et al. [46] investigated MIA on GANs, while Kong et al. [65] implemented MIA on the diffusion model. Yaghini et al. [66] explored the vulnerability of a subgroup under the MIA. In contrast, Conti et al. [57] investigated the vulnerability of one data point under multiple target models and MIAs. Nasr et al. [67] explored defenses against MIA with the adversarial training algorithm, while Jia et al. [68] proposed to find adversarial examples of the attack model.

### B. The Attacks against Spiking Neural Network

Works explored adversarial examples and backdoor attacks against SNNs. Abad et al. [70] systematically investigated the backdoor attack against the SNN. Specifically, they explored the trigger position, polarity, and size while inserting the same static trigger for all frames of a data point. To improve the moving backdoor in previous work [71], the authors conducted a complete experimental setup to find the best moving trigger, which changes the location over different frames. Besides, they proposed a smart backdoor to detect the most active region and insert moving triggers with the least used polarity in this region. Finally, they investigated dynamic moving backdoors where the triggers are invisible and unique for each image and frame via optimizing a spiking autoencoder to generate noise during SNN training.

Nomura et al. [72] explored the robustness of the time-to-first-spike encoding SNNs against white-box adversarial examples. Their result indicated the time-to-first-spike encoding SNNs are more robust than ANNs when trained with an appropriate temporal penalty setting, specifying the output spikes’ timing to approximate the reference timing. Sharmin et al. [73] systematically analyzed the adversarial robustness of SNNs and concluded the dependence of robustness on the SNN training mechanism.

To apply a gradient-based adversarial attack on SNNs trained with backpropagation and a surrogate activation neuron, Liang et al. [74] proposed two strategies to solve the problem of gradient-input incompatibility and gradient vanishing. Specifically, they designed a gradient-to-spike (G2S) converter to convert continuous gradients to ternary ones compatible with spike inputs. Then, they proposed a restricted spike flipper (RSF) to construct ternary gradients that can randomly flip the spike inputs when facing all-zero gradient maps, where the turnover rate of inputs is controllable.

## VII. CONCLUSIONS AND FUTURE WORK

This work evaluates the membership privacy leakage of SNNs with eight MIAs and compares the vulnerability of SNNs and ANNs when facing MIAs. Our results show that SNNs suffer from MIAs, especially when trained with neuromorphic datasets, where SNNs are more vulnerable than ANNs. If we convert ANNs to SNNs, the accuracy of MIAs will drop with a relatively low reduction in the accuracy of the original classification task. Hence, we recommend converting from ANNs to SNNs to reduce the leakage of membership privacy. The rule that a higher generalization gap usually leads

TABLE VI: The accuracy change while applying augmentation to static datasets.

Dataset	Model	Training Strategy	Without Augmentation				With Augmentation			
			Target Test Acc	Target Train Acc	MIA with Highest Acc		Target Test Acc	Target Train Acc	MIA with Highest Acc	
					MIA	Acc			MIA	Acc
CIFAR-10	ANN (VGG11)	BP	80.5%	100.0%	Mentr with confidence scores	70.3%	87.6%	98.6%	loss	59.5%
	SNN (VGG11)	BP	78.3%	99.6%	loss	69.5%	67.3%	67.6%	logit-scaled fire rate	51.7%
	SNN (VGG11)	Conversion	77.0%	97.4%	logit-scaled fire rate	63.1%	63.6%	70.5%	prediction correctness	53.3%
Caltech101	ANN (VGG11)	BP	61.8%	99.9%	logit-scaled confidence	80.2%	62.9%	91.9%	prediction correctness	60.5%
	SNN (VGG11)	BP	47.5%	45.1%	maximum fire rate	52.3%	30.4%	33.0%	avg membrane potential	51.7%
	SNN (VGG11)	Conversion	55.5%	99.1%	loss	72.9%	44.0%	70.6%	loss	66.4%

TABLE VII: The accuracy change while applying augmentation to neuromorphic datasets.

Dataset	Model	Without Augmentation				With EventDrop [61]				With NDA [56]			
		Target Test Acc	Target Train Acc	MIA with Highest Acc		Target Test Acc	Target Train Acc	MIA with Highest Acc		Target Test Acc	Target Train Acc	MIA with Highest Acc	
				MIA	Acc			MIA	Acc			MIA	Acc
CIFAR10-DVS	ANN (VGG11)	55.0%	100.0%	hinge loss	83.8%	55.1%	89.3%	logit-scaled confidence	86.5%	63.7%	95.1%	Mentr with confidence scores	71.8%
	SNN (VGG11)	61.8%	99.3%	Mentr with fire rates	83.9%	60.8%	90.3%	Mentr with fire rates	75.6%	61.4%	68.3%	Mentr with fire rates	58.3%
N-Caltech101	ANN (VGG11)	56.9%	100.0%	loss	78.6%	55.8%	88.7%	hinge loss	79.4%	60.7%	99.4%	loss	76.9%
	SNN (VGG11)	44.6%	80.0%	loss	79.5%	35.2%	37.0%	loss	55.2%	32.0%	32.1%	top-3 fire rates	53.8%

to a higher performance of MIAs is also applicable to SNNs from our exploration of various datasets, model types, and the hyperparameter study. Moreover, the basic data augmentation for static datasets and two recent data augmentation methods for neuromorphic datasets can improve the generalization of SNNs and eliminate MIAs. However, data augmentations cannot completely prevent MIAs. As the training accuracy of SNNs with data augmentation is usually lower than those without augmentation, we leave the method to reduce the generalization gap and keep the training accuracy of SNNs for future work. Finally, considering that SNNs are vulnerable to MIAs, we plan to investigate further on possible defense mechanisms.

## REFERENCES

- [1] I. Goodfellow, Y. Bengio, and A. Courville, *Deep Learning*. The MIT Press, 2016.
- [2] Y. Taigman, M. Yang, M. Ranzato, and L. Wolf, “Deepface: Closing the gap to human-level performance in face verification,” in *2014 IEEE Conference on Computer Vision and Pattern Recognition, CVPR 2014, Columbus, OH, USA, June 23-28, 2014*. IEEE Computer Society, June 2014, pp. 1701–1708. [Online]. Available: <https://doi.org/10.1109/CVPR.2014.220>
- [3] Z. Zou, K. Chen, Z. Shi, Y. Guo, and J. Ye, “Object detection in 20 years: A survey,” *Proceedings of the IEEE*, vol. 111, no. 3, pp. 257–276, 2023.
- [4] M. Pfeiffer and T. Pfeil, “Deep learning with spiking neurons: opportunities and challenges,” *Frontiers in neuroscience*, vol. 12, p. 409662, 2018.
- [5] F. Akopyan, J. Sawada, A. Cassidy, R. Alvarez-Icaza, J. Arthur, P. Merolla, N. Imam, Y. Nakamura, P. Datta, G.-J. Nam, B. Taba, M. Beakes, B. Brezzo, J. B. Kuang, R. Manohar, W. P. Risk, B. Jackson, and D. S. Modha, “Truenorth: Design and tool flow of a 65 mw 1 million neuron programmable neurosynaptic chip,” *IEEE Transactions on Computer-Aided Design of Integrated Circuits and Systems*, vol. 34, no. 10, pp. 1537–1557, 2015.
- [6] M. Davies, N. Srinivasa, T.-H. Lin, G. Chinya, Y. Cao, S. H. Choday, G. Dimou, P. Joshi, N. Imam, S. Jain, Y. Liao, C.-K. Lin, A. Lines, R. Liu, D. Mathaikutty, S. McCoy, A. Paul, J. Tse, G. Venkataramanan, Y.-H. Weng, A. Wild, Y. Yang, and H. Wang, “Loihi: A neuromorphic manycore processor with on-chip learning,” *IEEE Micro*, vol. 38, no. 1, pp. 82–99, 2018.
- [7] G. Chen, H. Cao, J. Conradt, H. Tang, F. Rohrbein, and A. Knoll, “Event-based neuromorphic vision for autonomous driving: A paradigm shift for bio-inspired visual sensing and perception,” *IEEE Signal Processing Magazine*, vol. 37, no. 4, pp. 34–49, 2020.
- [8] H. Wang, Y.-F. Li, and K. Gryllias, “Brain-inspired spiking neural networks for industrial fault diagnosis: A survey, challenges, and opportunities,” *arXiv preprint arXiv:2401.02429*, 2023.
- [9] S. H. Choi, “Spiking neural networks for biomedical signal analysis,” *Biomedical Engineering Letters*, pp. 1–12, 2024.
- [10] L. Xiaoxue, Z. Xiaofan, Y. Xin, L. Dan, W. He, Z. Bowen, Z. Bohan, Z. Di, and W. Liqun, “Review of medical data analysis based on spiking neural networks,” *Procedia Computer Science*, vol. 221, pp. 1527–1538, 2023.
- [11] A. Tavanaei, M. Ghodrati, S. R. Kheradpisheh, T. Masquelier, and A. Maida, “Deep learning in spiking neural networks,” *Neural networks*, vol. 111, pp. 47–63, 2019.
- [12] L. Deng, Y. Wu, X. Hu, L. Liang, Y. Ding, G. Li, G. Zhao, P. Li, and Y. Xie, “Rethinking the performance comparison between snns and anns,” *Neural Networks*, vol. 121, pp. 294–307, 2020.
- [13] Y. Cao, Y. Chen, and D. Khosla, “Spiking deep convolutional neural networks for energy-efficient object recognition,” *International Journal of Computer Vision*, vol. 113, pp. 54–66, 2015.
- [14] P. U. Diehl, D. Neil, J. Binas, M. Cook, S.-C. Liu, and M. Pfeiffer, “Fast-classifying, high-accuracy spiking deep networks through weight and threshold balancing,” in *2015 International joint conference on neural networks (IJCNN)*. Los Alamitos, CA, USA: IEEE Computer Society, 2015, pp. 1–8.
- [15] B. Rueckauer, I.-A. Lungu, Y. Hu, M. Pfeiffer, and S.-C. Liu, “Conversion of continuous-valued deep networks to efficient event-driven networks for image classification,” *Frontiers in neuroscience*, vol. 11, p. 294078, 2017.
- [16] A. Sengupta, Y. Ye, R. Wang, C. Liu, and K. Roy, “Going deeper in spiking neural networks: Vgg and residual architectures,” *Frontiers in Neuroscience*, vol. 13, 2019.
- [17] W. Fang, Z. Yu, Y. Chen, T. Huang, T. Masquelier, and Y. Tian,

- “Deep residual learning in spiking neural networks,” *Advances in Neural Information Processing Systems*, vol. 34, pp. 21 056–21 069, 2021.
- [18] E. Hunsberger and C. Eliasmith, “Spiking deep networks with LIF neurons,” *CoRR*, vol. abs/1510.08829, 2015.
  - [19] J. H. Lee, T. Delbruck, and M. Pfeiffer, “Training deep spiking neural networks using backpropagation,” *Frontiers in Neuroscience*, vol. 10, 2016.
  - [20] F. Lei, X. Yang, J. Liu, R. Dou, and N. Wu, “Dt-scnn: dual-threshold spiking convolutional neural network with fewer operations and memory access for edge applications,” *Frontiers in Computational Neuroscience*, vol. 18, p. 1418115, 2024.
  - [21] I. G. P. TEAM, *EU General Data Protection Regulation (GDPR): An Implementation and Compliance Guide - Second edition*, 2nd ed. IT Governance Publishing, 2017. [Online]. Available: <http://www.jstor.org/stable/j.ctt1trkk7x>
  - [22] P. BUKATY, *The California Consumer Privacy Act (CCPA): An implementation guide*. IT Governance Publishing, 2019. [Online]. Available: <http://www.jstor.org/stable/j.ctvjghvnn>
  - [23] R. E. Turkson, H. Qu, C. B. Mawuli, and M. J. Eghan, “Classification of alzheimer’s disease using deep convolutional spiking neural network,” *Neural Processing Letters*, vol. 53, no. 4, pp. 2649–2663, 2021.
  - [24] Y. Long, L. Wang, D. Bu, V. Bindschaedler, X. Wang, H. Tang, C. A. Gunter, and K. Chen, “A pragmatic approach to membership inferences on machine learning models,” in *2020 IEEE European Symposium on Security and Privacy (EuroS&P)*. Los Alamitos, CA, USA: IEEE Computer Society, 2020, pp. 521–534.
  - [25] D. Auge, J. Hille, E. Mueller, and A. Knoll, “A survey of encoding techniques for signal processing in spiking neural networks,” *Neural Processing Letters*, vol. 53, no. 6, pp. 4693–4710, 2021.
  - [26] R. Shokri, M. Stronati, C. Song, and V. Shmatikov, “Membership inference attacks against machine learning models,” in *Proceedings of the 38th IEEE Symposium on Security and Privacy, SP 2017, San Jose, CA, USA, May 22-26, 2017*. Los Alamitos, CA, USA: IEEE Computer Society, May 2017, pp. 3–18.
  - [27] A. Salem, Y. Zhang, M. Humbert, P. Berrang, M. Fritz, and M. Backes, “ML-leaks: Model and data independent membership inference attacks and defenses on machine learning models,” in *Proceedings of the 26th Annual Network and Distributed System Security Symposium, NDSS 2019, San Diego, California, USA, February 24-27, 2019*. Reston, Virginia, USA: The Internet Society, February 2019.
  - [28] N. Carlini, S. Chien, M. Nasr, S. Song, A. Terzis, and F. Tramèr, “Membership inference attacks from first principles,” in *Proceedings of the 43rd IEEE Symposium on Security and Privacy, SP 2022, San Francisco, CA, USA, May 22-26, 2022*. Los Alamitos, CA, USA: IEEE Computer Society, 2022, pp. 1897–1914.
  - [29] D. Połap, M. Woźniak, W. Hołubowski, and R. Damaševičius, “A heuristic approach to the hyperparameters in training spiking neural networks using spike-timing-dependent plasticity,” *Neural Computing and Applications*, vol. 34, no. 16, pp. 13 187–13 200, 2022.
  - [30] B. Rueckauer, I.-A. Lungu, Y. Hu, and M. Pfeiffer, “Theory and tools for the conversion of analog to spiking convolutional neural networks,” *arXiv preprint arXiv:1612.04052*, 2016.
  - [31] E. Izhikevich, “Simple model of spiking neurons,” *IEEE Transactions on Neural Networks*, vol. 14, no. 6, pp. 1569–1572, 2003.
  - [32] R. M. Borisyuk and G. N. Borisyuk, “Information coding on the basis of synchronization of neuronal activity,” *BioSystems*, vol. 40, no. 1-2, pp. 3–10, 1997.
  - [33] S. Dutta, V. Kumar, A. Shukla, N. R. Mohapatra, and U. Ganguly, “Leaky integrate and fire neuron by charge-discharge dynamics in floating-body mosfet,” *Scientific reports*, vol. 7, no. 1, p. 8257, 2017.
  - [34] W. Gerstner, W. M. Kistler, R. Naud, and L. Paninski, *Neuronal dynamics: From single neurons to networks and models of cognition*. Cambridge: Cambridge University Press, 2014.
  - [35] W. Fang, Z. Yu, Y. Chen, T. Masquelier, T. Huang, and Y. Tian, “Incorporating learnable membrane time constant to enhance learning of spiking neural networks,” in *2021 IEEE/CVF International Conference on Computer Vision (ICCV)*. Los Alamitos, CA, USA: IEEE Computer Society, oct 2021, pp. 2641–2651.
  - [36] E. O. Neftci, H. Mostafa, and F. Zenke, “Surrogate gradient learning in spiking neural networks: Bringing the power of gradient-based optimization to spiking neural networks,” *IEEE Signal Processing Magazine*, vol. 36, no. 6, pp. 51–63, 2019.
  - [37] W. Fang, Y. Chen, J. Ding, Z. Yu, T. Masquelier, D. Chen, L. Huang, H. Zhou, G. Li, and Y. Tian, “Spikingjelly: An open-source machine learning infrastructure platform for spike-based intelligence,” *Science Advances*, vol. 9, no. 40, p. eadi1480, 2023.
  - [38] D. P. Kingma and J. Ba, “Adam: A method for stochastic optimization,” in *Proceedings of the 3rd International Conference on Learning Representations*, ser. ICLR 2015, 2015.
  - [39] S. Ruder, “An overview of gradient descent optimization algorithms,” *arXiv preprint arXiv:1609.04747*, 2016.
  - [40] M. Nasr, R. Shokri, and A. Houmansadr, “Comprehensive privacy analysis of deep learning: Passive and active white-box inference attacks against centralized and federated learning,” in *2019 IEEE symposium on security and privacy (SP)*. Los Alamitos, CA, USA: IEEE Computer Society, 2019, pp. 739–753.
  - [41] A. Sablayrolles, M. Douze, C. Schmid, Y. Ollivier, and H. Jégou, “White-box vs black-box: Bayes optimal strategies for membership inference,” in *Proceedings of the 36th International Conference on Machine Learning, ICML 2019, Long Beach, California, USA, 9-15 June 2019*. PMLR, June 2019, pp. 5558–5567.
  - [42] C. A. Choquette-Choo, F. Tramer, N. Carlini, and N. Papernot, “Label-only membership inference attacks,” in *Proceedings of the 38th International Conference on Machine Learning, ICML 2021, Virtual Event, July 18-24, 2021*, vol. 139. PMLR, July 2021, pp. 1964–1974.
  - [43] M. Conti, J. Li, S. Picek, and J. Xu, “Label-only membership inference attack against node-level graph neural networks,” in *Proceedings of the 15th ACM Workshop on Artificial Intelligence and Security, AISec 2022, Los Angeles, CA, USA, November 7, 2022*. New York, NY, USA: Association for Computing Machinery, November 2022, p. 1–12.
  - [44] X. He and Y. Zhang, “Quantifying and mitigating privacy risks of contrastive learning,” in *Proceedings of the 2021 ACM SIGSAC Conference on Computer and Communications Security, CCS 2021, Virtual Event, Republic of Korea, November 15 - 19, 2021*, Y. Kim, J. Kim, G. Vigna, and E. Shi, Eds. New York, NY, USA: Association for Computing Machinery, November 2021, pp. 845–863.
  - [45] H. Liu, J. Jia, W. Qu, and N. Z. Gong, “Encodermi: Membership inference against pre-trained encoders in contrastive learning,” in *Proceedings of the 2021 ACM SIGSAC Conference on Computer and Communications Security, CCS 2021, Virtual Event, Republic of Korea, November 15 - 19, 2021*. New York, NY, USA: Association for Computing Machinery, November 2021, p. 2081–2095.
  - [46] J. Hayes, L. Melis, G. Danezis, and E. D. Cristofaro, “LOGAN: Membership inference attacks against generative models,” *Proceedings on Privacy Enhancing Technologies*, vol. 2019, pp. 133–152, 2019.
  - [47] S. Yeom, I. Giacomelli, M. Fredrikson, and S. Jha, “Privacy risk in machine learning: Analyzing the connection to overfitting,” in *Proceedings of the 31st IEEE Computer Security Foundations Symposium, CSF 2018, Oxford, United Kingdom, July 9-12, 2018*. Los Alamitos, CA, USA: IEEE Computer Society, July 2018, pp. 268–282.
  - [48] J. Ye, A. Maddi, S. K. Murakonda, V. Bindschaedler, and R. Shokri, “Enhanced membership inference attacks against machine learning models,” in *Proceedings of the 2022 ACM SIGSAC Conference on Computer and Communications Security, ser. CCS ’22*. New York, NY, USA: Association for Computing Machinery, 2022, p. 3093–3106.
  - [49] B. Hui, Y. Yang, H. Yuan, P. Burlina, N. Z. Gong, and Y. Cao, “Practical blind membership inference attack via differential comparisons,” in *28th Annual Network and Distributed System Security Symposium, NDSS 2021, virtually, February 21-25, 2021*. Reston, Virginia, USA: The Internet Society, 2021.
  - [50] L. Song and P. Mittal, “Systematic evaluation of privacy risks of machine learning models,” in *Proceedings of the 30th USENIX Security Symposium, USENIX Security 2021, Virtual Event, August 11-13, 2021*. Berkeley, CA, USA: USENIX Association, August 2021, pp. 2615–2632.
  - [51] G. Orchard, A. Jayawant, G. K. Cohen, and N. Thakor, “Converting static image datasets to spiking neuromorphic datasets using saccades,” *Frontiers in neuroscience*, vol. 9, p. 437, 2015.
  - [52] H. Li, H. Liu, X. Ji, G. Li, and L. Shi, “Cifar10-dvs: an event-stream dataset for object classification,” *Frontiers in neuroscience*, vol. 11, p. 309, 2017.
  - [53] K. Simonyan and A. Zisserman, “Very deep convolutional networks for large-scale image recognition,” *arXiv preprint arXiv:1409.1556*, 2014.
  - [54] K. He, X. Zhang, S. Ren, and J. Sun, “Deep residual learning for image recognition,” in *Proceedings of the IEEE conference on computer vision and pattern recognition*. Los Alamitos, CA, USA: IEEE Computer Society, 2016, pp. 770–778.

- [55] A. Krizhevsky, I. Sutskever, and G. E. Hinton, "Imagenet classification with deep convolutional neural networks," *Advances in neural information processing systems*, vol. 25, 2012.
- [56] Y. Li, Y. Kim, H. Park, T. Geller, and P. Panda, "Neuromorphic data augmentation for training spiking neural networks," in *Computer Vision – ECCV 2022: 17th European Conference, Tel Aviv, Israel, October 23–27, 2022, Proceedings, Part VII*. Berlin, Heidelberg: Springer-Verlag, 2022, p. 631–649.
- [57] M. Conti, J. Li, and S. Picek, "On the vulnerability of data points under multiple membership inference attacks and target models," *arXiv preprint arXiv:2210.16258*, 2022.
- [58] N. Fourcaud-Trocmé, D. Hansel, C. Van Vreeswijk, and N. Brunel, "How spike generation mechanisms determine the neuronal response to fluctuating inputs," *Journal of neuroscience*, vol. 23, no. 37, pp. 11 628–11 640, 2003.
- [59] E. M. Izhikevich, "Simple model of spiking neurons," *IEEE Transactions on neural networks*, vol. 14, no. 6, pp. 1569–1572, 2003.
- [60] Y. Wu, L. Deng, G. Li, J. Zhu, and L. Shi, "Spatio-temporal backpropagation for training high-performance spiking neural networks," *Frontiers in Neuroscience*, vol. 12, 2018.
- [61] F. Gu, W. Sng, X. Hu, and F. Yu, "Eventdrop: Data augmentation for event-based learning," *arXiv preprint arXiv:2106.05836*, 2021.
- [62] T. DeVries and G. W. Taylor, "Improved regularization of convolutional neural networks with cutout," *arXiv preprint arXiv:1708.04552*, 2017.
- [63] S. Yun, D. Han, S. J. Oh, S. Chun, J. Choe, and Y. Yoo, "Cutmix: Regularization strategy to train strong classifiers with localizable features," in *Proceedings of the IEEE/CVF international conference on computer vision*. Los Alamitos, CA, USA: IEEE Computer Society, 2019, pp. 6023–6032.
- [64] Z. Li and Y. Zhang, "Membership leakage in label-only exposures," in *Proceedings of the 2021 ACM SIGSAC Conference on Computer and Communications Security, CCS 2021, Virtual Event, Republic of Korea, November 15 - 19, 2021*. New York, NY, USA: Association for Computing Machinery, 2021, p. 880–895.
- [65] F. Kong, J. Duan, R. Ma, H. Shen, X. Zhu, X. Shi, and K. Xu, "An efficient membership inference attack for the diffusion model by proximal initialization," *arXiv preprint arXiv:2305.18355*, 2023.
- [66] M. Yaghini, B. Kulynych, G. Cherubin, and C. Troncoso, "Disparate vulnerability: On the unfairness of privacy attacks against machine learning," *Proceedings on Privacy Enhancing Technologies*, pp. 460–480, 2022.
- [67] M. Nasr, R. Shokri, and A. Houmansadr, "Machine learning with membership privacy using adversarial regularization," in *Proceedings of the 25th ACM SIGSAC Conference on Computer and Communications Security, CCS 2018, Toronto, ON, Canada, October 15-19, 2018*. New York, NY, USA: Association for Computing Machinery, 2018, pp. 634–646.
- [68] J. Jia, A. Salem, M. Backes, Y. Zhang, and N. Z. Gong, "MemGuard: Defending against black-box membership inference attacks via adversarial examples," in *Proceedings of the 26th ACM SIGSAC Conference on Computer and Communications Security, CCS 2019, London, UK, November 11-15, 2019*. New York, NY, USA: Association for Computing Machinery, 2019, pp. 259–274.
- [69] Z. Chen and K. Pattabiraman, "Overconfidence is a dangerous thing: Mitigating membership inference attacks by enforcing less confident prediction," *arXiv preprint arXiv:2307.01610*, 2023.
- [70] G. Abad, O. Ersoy, S. Picek, and A. Urbiet, "Sneaky spikes: Uncovering stealthy backdoor attacks in spiking neural networks with neuromorphic data," in *NDSS*, 2024.
- [71] G. Abad, O. Ersoy, S. Picek, V. J. Ramírez-Durán, and A. Urbiet, "Poster: Backdoor attacks on spiking nns and neuromorphic datasets," in *Proceedings of the 2022 ACM SIGSAC Conference on Computer and Communications Security*, ser. CCS '22. New York, NY, USA: Association for Computing Machinery, 2022, p. 3315–3317.
- [72] O. Nomura, Y. Sakemi, T. Hosomi, and T. Morie, "Robustness of spiking neural networks based on time-to-first-spike encoding against adversarial attacks," *IEEE Transactions on Circuits and Systems II: Express Briefs*, vol. 69, no. 9, pp. 3640–3644, 2022.
- [73] S. Sharmin, P. Panda, S. S. Sarwar, C. Lee, W. Ponghiran, and K. Roy, "A comprehensive analysis on adversarial robustness of spiking neural networks," in *2019 International Joint Conference on Neural Networks (IJCNN)*. Los Alamitos, CA, USA: IEEE Computer Society, 2019, pp. 1–8.
- [74] L. Liang, X. Hu, L. Deng, Y. Wu, G. Li, Y. Ding, P. Li, and Y. Xie, "Exploring adversarial attack in spiking neural networks with spike-compatible gradient," *IEEE transactions on neural networks and learning systems*, vol. 34, no. 5, pp. 2569–2583, 2021.

## APPENDIX

### A. MIAs against SNNs

Table VIII provides the attack accuracy of eight MIAs against SNNs trained with various model types and datasets. The training strategy "bp" means backpropagation, and "conversion" means converting ANNs to obtain SNNs. "Target Test Acc" and "Target Train Acc" represent the test and training accuracy of the target model. Note that the accuracy of the shadow model is close to the accuracy of the target model as the shadow model mimics the target model. We explain eight MIAs and how to apply them in Section III-C.

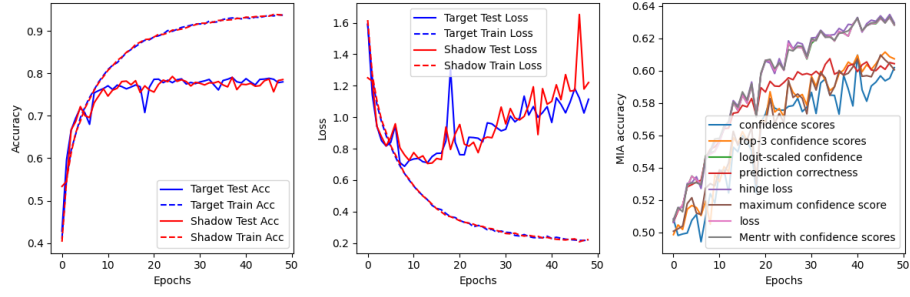
### B. MIAs against ANNs

Table IX provides the attack accuracy of eight MIAs against ANNs trained with various model types and datasets. The meaning of each column is the same as for Table VIII.

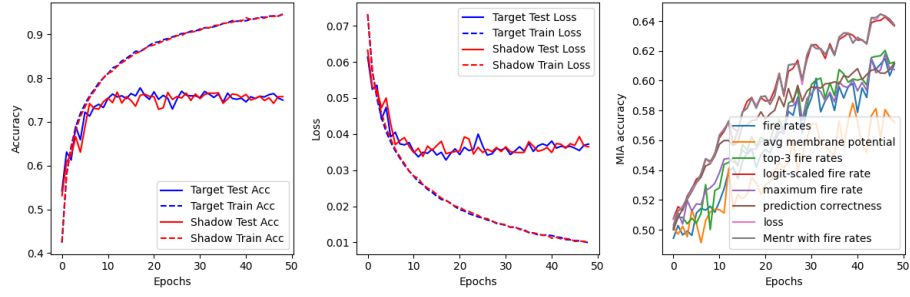
### C. Accuracy vs. Training Epochs

Figure 5 shows how the loss, accuracy, and attack accuracy change during the training epochs of the target and shadow models. In the first image of each sub-figure, we draw the change of the training and test accuracy of target and shadow models. Each sub-figure's second image describes the loss modification during the training. The last image of each sub-figure shows the change in attack accuracy within MIAs explored in this work. Each sub-figure is related to a dataset and model type.

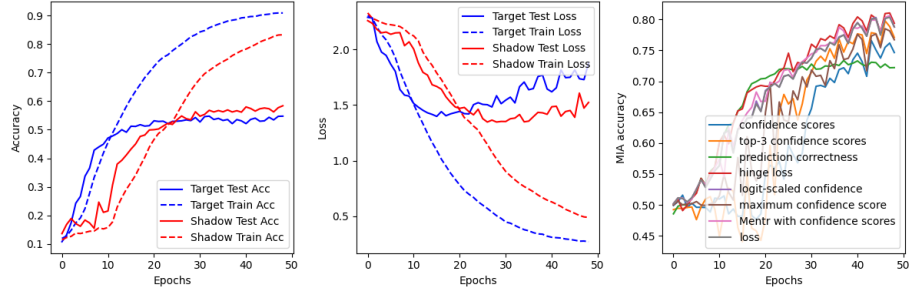




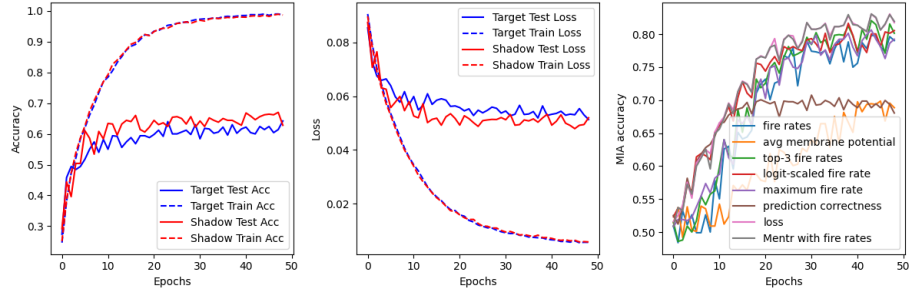
(a) ANN (CNN) and CIFAR-10



(b) SNN (CNN) and CIFAR-10



(c) ANN (CNN) and CIFAR10-DVS



(d) SNN (CNN) and CIFAR10-DVS

Fig. 5: The modification of the accuracy of the original task, loss, and attack accuracy of MIAs along the training epochs.

TABLE VIII: The attack accuracy of MIAs against SNNs.

Dataset	Model Type	Training Strategy	Target Test Acc	Target Train Acc	Attack Accuracy of MIAs							
					fire rates	loss	prediction correctness	top-3 fire rates	maximum fire rate	logit-scaled fire rate	Mentr with fire rates	avg membrane potential
MNIST	SNN (CNN)	Bp	99.4%	99.9%	50.2%	51.0%	50.3%	50.0%	50.7%	51.0%	51.0%	50.7%
N-MNIST	SNN (CNN)	Bp	99.2%	99.9%	51.0%	52.7%	50.4%	49.3%	52.4%	52.7%	52.7%	48.1%
MNIST	SNN (CNN)	Conversion	99.4%	99.9%	50.0%	51.2%	50.4%	50.8%	51.1%	51.2%	51.2%	50.2%
MNIST	SNN (VGG11)	Bp	99.3%	99.9%	50.2%	51.1%	50.3%	50.9%	50.8%	51.1%	51.2%	50.1%
N-MNIST	SNN (VGG11)	Bp	99.0%	99.9%	50.5%	51.9%	50.5%	49.3%	49.4%	49.6%	52.0%	50.0%
MNIST	SNN (VGG11)	Conversion	99.1%	99.9%	49.7%	50.5%	50.5%	50.2%	50.1%	50.1%	50.5%	49.5%
CIFAR-10	SNN (CNN)	Bp	78.9%	96.6%	63.5%	65.9%	59.8%	64.0%	63.2%	65.9%	65.9%	59.1%
CIFAR10-DVS	SNN (CNN)	Bp	64.4%	99.5%	79.7%	83.6%	67.9%	83.1%	79.7%	82.4%	83.6%	69.3%
CIFAR-10	SNN (CNN)	Conversion	54.9%	66.3%	54.3%	56.3%	56.5%	52.2%	51.4%	56.3%	56.4%	51.6%
CIFAR-10	SNN (VGG11)	Bp	78.3%	99.6%	67.4%	69.5%	60.7%	67.8%	67.4%	69.3%	69.5%	47.3%
CIFAR10-DVS	SNN (VGG11)	Bp	61.8%	99.3%	78.9%	83.8%	69.3%	82.5%	81.4%	82.3%	83.9%	50.3%
CIFAR-10	SNN (VGG11)	Conversion	77.0%	97.4%	52.5%	61.6%	60.4%	56.7%	58.4%	63.1%	61.6%	49.2%
CIFAR-10	SNN (ResNet18)	Bp	72.0%	98.6%	65.7%	69.4%	63.6%	66.2%	65.6%	69.4%	69.4%	51.8%
CIFAR10-DVS	SNN (ResNet18)	Bp	49.4%	100.0%	90.4%	87.7%	75.4%	92.2%	91.3%	92.8%	87.9%	60.1%
CIFAR-10	SNN (ResNet18)	Conversion	74.0%	94.2%	58.2%	61.3%	59.8%	58.8%	58.9%	61.2%	61.4%	50.2%
Caltech101	SNN (CNN)	Bp	71.0%	99.9%	65.9%	74.1%	64.4%	73.7%	73.0%	74.1%	74.1%	56.0%
N-Caltech101	SNN (CNN)	Bp	68.0%	99.6%	74.8%	78.8%	65.8%	78.8%	78.1%	78.9%	78.8%	55.5%
Caltech101	SNN (CNN)	Conversion	51.6%	77.4%	50.0%	67.5%	67.8%	60.2%	62.0%	67.6%	67.5%	50.1%
Caltech101	SNN (VGG11)	Bp	47.5%	45.1%	50.0%	52.0%	49.8%	50.6%	52.3%	49.4%	49.5%	49.3%
N-Caltech101	SNN (VGG11)	Bp	44.6%	80.0%	50.0%	79.5%	70.3%	65.2%	64.9%	70.2%	70.2%	49.6%
Caltech101	SNN (VGG11)	Conversion	55.5%	99.1%	56.0%	72.9%	70.8%	70.4%	70.7%	74.2%	72.9%	50.0%
Caltech101	SNN (ResNet18)	Bp	65.7%	99.9%	78.9%	78.1%	67.2%	85.5%	85.4%	85.0%	79.4%	53.2%
N-Caltech101	SNN (ResNet18)	Bp	64.4%	100.0%	74.8%	78.3%	67.9%	78.6%	76.6%	75.8%	79.4%	53.1%
Caltech101	SNN (ResNet18)	Conversion	59.0%	99.8%	61.2%	72.9%	69.7%	67.4%	69.4%	72.9%	72.9%	53.4%

TABLE IX: The attack accuracy of MIAs against ANNs.

Dataset	Model Type	Training Strategy	Target Test Acc	Target Train Acc	Attack Accuracy of MIAs							
					confidence scores	loss	prediction correctness	top-3 confidence scores	maximum confidence score	logit-scaled confidence	Mentr with confidence scores	hinge loss
MNIST	ANN (CNN)	Bp	99.3%	99.8%	49.5%	51.1%	50.3%	50.8%	51.2%	51.2%	51.2%	51.2%
N-MNIST	ANN (CNN)	Bp	98.6%	99.4%	51.3%	51.5%	50.6%	49.1%	51.5%	51.5%	51.4%	51.6%
MNIST	ANN (VGG11)	Bp	99.4%	100.0%	50.2%	51.0%	50.3%	50.6%	51.0%	51.0%	51.0%	50.8%
N-MNIST	ANN (VGG11)	Bp	98.9%	100.0%	50.4%	51.6%	50.5%	51.3%	51.5%	51.6%	51.6%	51.6%
CIFAR-10	ANN (CNN)	Bp	80.8%	99.4%	65.2%	68.0%	59.6%	66.7%	66.9%	68.0%	68.0%	68.1%
CIFAR10-DVS	ANN (CNN)	Bp	56.2%	87.4%	62.2%	73.5%	71.4%	69.7%	69.9%	73.5%	72.9%	73.5%
CIFAR-10	ANN (VGG11)	Bp	80.5%	100.0%	61.2%	70.1%	60.0%	66.5%	69.1%	70.1%	70.3%	70.2%
CIFAR10-DVS	ANN (VGG11)	Bp	55.0%	100.0%	76.6%	83.6%	72.3%	79.6%	81.6%	83.6%	83.4%	83.8%
CIFAR-10	ANN (ResNet18)	Bp	82.0%	100.0%	63.9%	72.8%	59.0%	69.3%	72.1%	72.8%	72.9%	72.7%
CIFAR10-DVS	ANN (ResNet18)	Bp	57.9%	100.0%	79.0%	84.3%	72.3%	70.8%	82.2%	84.3%	84.2%	84.2%
Caltech101	ANN (CNN)	Bp	71.4%	93.9%	68.4%	69.6%	64.2%	69.6%	69.6%	69.7%	68.4%	69.4%
N-Caltech101	ANN (CNN)	Bp	61.0%	99.2%	70.0%	80.0%	69.6%	79.1%	79.7%	80.0%	79.7%	79.9%
Caltech101	ANN (VGG11)	Bp	61.8%	99.9%	58.6%	79.6%	69.2%	78.2%	79.4%	80.2%	79.9%	79.5%
N-Caltech101	ANN (VGG11)	Bp	56.9%	100.0%	67.7%	78.6%	71.6%	76.1%	77.7%	78.6%	78.6%	78.5%
Caltech101	ANN (ResNet18)	Bp	66.1%	99.9%	50.0%	77.5%	66.8%	78.0%	77.1%	77.7%	77.8%	78.5%
N-Caltech101	ANN (ResNet18)	Bp	59.4%	100.0%	63.7%	79.2%	70.4%	74.4%	78.5%	79.2%	79.2%	79.3%